Reactions of the Tetrachlorobis(imidazole)ruthenium(III) and Pentachloro(imidazole)ruthenium(III) Anions with Imidazole and *N6,N6*-Dimethyladenine

Craig Anderson and André L. Beauchamp*

Département de Chimie, Université de Montréal, Montréal, Québec, Canada H3C 3J7

Received October 28, 1994[⊗]

The reactions of $(ImH)_2[RuCl_5Im]$ (Im = imidazole) in water were monitored by ^1H NMR spectroscopy. Fast initial aquation of $[RuCl_5Im]^{2-}$ to $[RuCl_4(H_2O)Im]^-$ is followed by successive substitutions along two pathways: slow displacement of extra Cl^- ligands by water to form higher aquation products and attack of an Im ligand to give $[RuCl_4Im_2]^-$, which then aquates. In the presence of 2 equiv of added Im, $(ImH)[RuCl_4Im_2]$ gives mixtures of complexes containing three to four Im per Ru, whereas 20 equiv lead to species with five to six Im per Ru. Imidazole-rich species coexist in solution with the starting $[RuCl_4Im_2]^-$ ion. X-ray diffraction work on $[Ru(OH)_2Im_4][RuCl_4Im_2]$ (monoclinic, $P2_1/c$, a = 13.126 Å, b = 10.8833 Å, c = 10.6110 Å, β = 108.28°, R = 0.045) shows the presence of octahedral *trans*-$[Ru(OH)_2Im_4]^+$ and *trans*-$[RuCl_4Im_2]^-$ connected by hydrogen bonding. Many complexes and aquation products successively appear when Im is reacted with $(ImH)_2[RuCl_5Im]$, and species with five to six Im ligands per Ru are again obtained with 20 equiv of added Im. An end product is isolated as yellow crystals and shown by X-ray diffraction (hexagonal, $P6_3/m$, a = 8.9756 Å, c = 20.880 Å, R = 0.023) to be the $[RuIm_6]CO_3 \cdot 5H_2O$ compound, containing the reduced Ru(II) octahedral $[RuIm_6]^{2+}$. In the presence of *N6,N6*-dimethyladenine (DMAD), $[RuCl_4Im_2]^-$ in water slowly forms the $[RuCl_3Im_2(DMAD)]$ complex, in which the adenine ligand is monodentate.

Introduction

A previous paper from this laboratory[1] reported on the solvolysis of the antitumor compound $(ImH)[RuCl_4Im_2]$ (**1**, Im = imidazole)[2] in methanol, dimethyl sulfoxide (DMSO), and

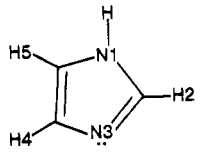

Im

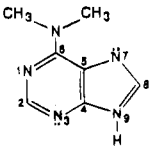

DMAD

water. Chloride displacement by solvent molecules could be monitored by ^1H NMR spectroscopy, despite the large line widths and huge chemical shifts due to the presence of the paramagnetic Ru(III) center.[3,4] In water, $[RuCl_4Im_2]^-$ (**1**) initially present was found to aquate to $[RuCl_3(H_2O)Im_2]$ (**1a**)[5] over several days. Further aquation to $[RuCl_2(H_2O)_2Im_2]^+$ (**1b1** and **1b2**) took place over several weeks, whereas a significant amount of $[RuCl(H_2O)_3Im_2]^{2+}$ (**1c**) was present only after a few months. Very recently, the same pattern was observed for the early aquation steps by Keppler and co-workers.[6] These results are in good agreement with earlier observations by Keppler's group[7] that the binding to biological substrates is slow in fresh solutions of $[RuCl_4Im_2]^-$ but much faster when aged solutions are used, suggesting that initial aquation to $[RuCl_3(H_2O)Im_2]$ is a prerequisite step.

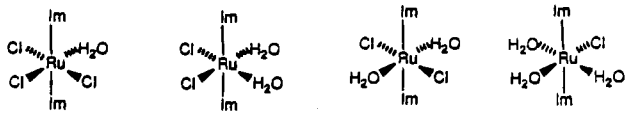

1a

1b1

1b2

1c

For the present study, a similar approach was first applied to follow the aquation of $(ImH)_2[RuCl_5Im]$ (**2**), a compound for which antitumor activity has also been reported.[8] The behavior of this system turned out to be much more complex, since a large number of species resulted from chloride displacement by the solvent and coordination of extra imidazole ligands. In a second step, the work was extended to solutions of $[RuCl_4Im_2]^-$ or $[RuCl_5Im]^{2-}$ containing a simple N-donor ligand. There is evidence that these Ru(III) species, like the active platinum agents, owe their antitumor properties to interactions taking place at the DNA level. Thus, a good understanding of their interactions in aqueous solution with the kind of binding sites present in DNA is crucial to unravel their mode of action and identify the active species.[9,10] Our efforts were first directed toward imidazole, which is present as such in biomolecules like histidine and as the five-membered ring of purines in DNA. It

* Author to whom correspondence should be addressed.

[⊗] Abstract published in *Advance ACS Abstracts,* November 1, 1995.

(1) Anderson, C.; Beauchamp, A. L. *Can. J. Chem.* **1995**, *73*, 471.
(2) Keppler, B. K.; Rupp, W.; Juhl, U. M.; Endres, H.; Niebl R.; Balzer. W. *Inorg. Chem.* **1987**, *26*, 4366.
(3) Bertini., I.; Luchinat, C. *NMR of Paramagnetic Molecules in Biological Systems*, Benjamin-Cummings: Menlo Park, CA, 1986. La Mar, G. N. In *NMR of Paramagnetic Molecules;* De Horricks, W., Jr., Holm, R. H., Eds.; Academic Press: New York, 1973.
(4) Satterlee, J. D. *Concepts Magn. Reson.* **1990**, *2*, 69; **1990**, *2*, 119.
(5) Under equilibrium conditions, aqua species may exist as mixtures of the Ru–OH_2 and Ru–OH forms, whose proportions are not known at the present time, since the two forms are in fast exchange on the NMR time scale and individual pk_a values have not been determined.
(6) Dhubhghaill, O. M. N.; Hagen, W. R.; Keppler, B. K.; Lipponer, K.-G.; Sadler, P. J. *J. Chem. Soc., Dalton Trans.* **1994**, 3305.
(7) Keppler, B. K.; Henn, M.; Juhl, U. M.; Berger, M. R.; Niebl, R.; Wagner, F. E. *Prog. Clin. Biochem. Med.* **1989**, *10*, 41. Kratz, F.; Keppler, B. K.; Messori, L.; Smith, C.; Baker, E. N. *Met.-Based Drugs* **1994**, *1*, 169. Kratz, F.; Hartmann, M.; Keppler, B. K.; Messori, L. *J. Biol. Chem.* **1994**, *269*, 2581.
(8) Keppler, B. K.; Wehe, D.; Endres. H.; Rupp, W. *Inorg. Chem.* **1987**, *26*, 844.
(9) Roberts, J. J.; Pera, M. F. In *Platinum, Gold and Other Chemotherapeutic Agents*; Lippard, S., Ed.; ACS Symposium Series 209; American Chemical Society: Washington, DC, 1983; p 335.
(10) Heijden, M.; van Vliet, P. M.; Haasnoot, J. G.; Reedijk, J. *J. Chem. Soc., Dalton Trans.* **1993**, 3675, and references cited therein.

0020-1669/95/1334-6065$09.00/0

is a particularly attractive ligand for the present study, because its ligating ability remains simple, while providing several protons to be probed by ^{1}H NMR spectroscopy. The complexation of imidazoles and purines to the $[Ru(NH_3)_5]^{3+}$ fragment has been thoroughly examined,[11,12] but these results are only moderately informative, because the kinetically inert $Ru-NH_3$ bond makes these systems much less complicated than the more labile chloro species considered here. Literature is also available on the reactions of imidazole with various Ru−Cl−sulfoxide antitumor agents,[13−18] which are largely concerned with the Ru(II) oxidation state, favored by the presence of the reducing sulfoxide ligand. Besides imidazole, *N6,N6*-dimethyladenine (or 6-(dimethylamino)purine, DMAD) was examined to exemplify the binding of a purine unit. Strictly speaking, this ligand is not a model for metal binding to purines in DNA, because the 6-NMe_2 group creates steric hindrance at the usual N(7) target and the purine should bind as the N(7)−H tautomer via the N(9) atom as noted with CH_3Hg^+.[19] Nevertheless, by preventing the formation of multiple monomeric and polymeric complexes, DMAD allowed us to cast some light on the behavior of an imidazolic site with a basicity typical of adenine or guanine.

Experimental Section

Instruments and Reactants. ^{1}H NMR spectra were recorded on Varian XL-300 or Bruker AMX-300 spectrometers. Sweep widths of 50 or 100 KHz were used at a pulse rate of 0.04 s. The peaks were referenced to the residual solvent peak (D_2O $\delta = 4.80$) and given with respect to Me_4Si, downfield being positive. Infrared spectra (220−4000 cm^{-1}) were recorded on a Perkin-Elmer 1600 FTIR apparatus as either KBr or CsI pellets. Microanalyses were done by the Guelph Chemical Laboratories, Guelph, Canada.

Imidazole was used as received from Aldrich. DMAD was prepared from 6-chloropurine (Aldrich) as described earlier.[20] $RuCl_3 \cdot 3H_2O$ (Aldrich) was "activated" by refluxing in an ethanol/aqueous HCl mixture for several hours prior to each run.

C(2)-deuterated imidazole was obtained by exchange with D_2O.[21] A solution of imidazole (1.0 g) in 10 mL of D_2O was sealed in a glass tube. After three freeze/pump/thaw cycles to remove dissolved gases, the solution was heated to 150 °C for 2 h and then cooled to room temperature. C(2)-deuteration of ~95% was determined from the relative intensity (1:70) of the ^{1}H NMR peaks for H(2) and H(4)/H(5), respectively. Partial C(2)-deuteration also took place over several weeks at room temperature in D_2O.

To obtain C(8)-deuterated dimethyladenine, 110 mg were dissolved in 5 mL of D_2O and refluxed anaerobically for 2.5 h. This solution was cooled and filtered. Almost complete deuteration at C(8) was indicated by ^{1}H NMR spectroscopy.

Table 1. Crystal Data

formula	$C_{18}H_{26}Cl_4N_{12}O_2Ru_2$	$C_{19}H_{34}N_{12}O_8Ru$
fw	786.43	659.62
space group	$P2_1/c$	$P6_3/m$
a, Å	13.126(3)	8.9756(13)
b, Å	10.8833(8)	8.9756
c, Å	10.6110(10)	20.880(3)
α, deg	90	90
β, deg	108.28(1)	90
γ, deg	90	120
V, Å^3	1439.3(4)	1456.8(3)
Z	2	2
T, K	293	293
λ, Å	1.541 78	1.541 78
D_{calc}, g cm^{-3}	1.815	1.504
μ, cm^{-1}	125.8	49.9
R^a	0.045	0.023
$R_w{}^a$	0.049	0.025

^{a} $R = \sum||F_o| - |F_c||/\sum|F_o|$; $R_w = [\sum w(|F_o| - |F_c|)^2/\sum w|F_o|^2]^{1/2}$.

(ImH)[$RuCl_4Im_2$] (**1**) was prepared as described in our previous paper.[1] $(ImH)_2[RuCl_5Im]$ (**2**) was obtained by the following variation of literature methods.[8,22] A solution containing 2.05 mL of concentrated HCl, 24 mL of water, 25 mL of EtOH, and 1.01 g of $RuCl_3 \cdot 3H_2O$ was refluxed for 2 h. The volume was reduced to 20 mL in open air, at which point it had turned red. The solution was cooled to room temperature and 2.52 g of imidazole in 5 mL of 6 M HCl were quickly added. The resulting solution was stirred for 5 min at room temperature. The volume was then reduced to two-thirds under vacuum, and the mixture was allowed to stand for 15 h at room temperature. Bright ruby red crystals had then appeared, which were filtered and washed with copious amounts of EtOH; yield 30%. Anal. Calcd for $C_9H_{14}Cl_5N_6Ru$: C, 22.31; H, 2.91; N, 17.34; Cl, 36.58. Found: C, 22.47; H, 3.00; N, 17.51; Cl, 36.93. IR data (KCl, cm^{-1}): 308 (vs, sh), 287 (s, split), 275 (w), 255 (w).

The relative intensities (1:1:1:2:4) of the signals at −27.0, −15.0, and −6.7 ppm (for the $[RuCl_4(H_2O)Im]^-$ species formed instantly from $[RuCl_5Im]^{2-}$, see text) and at 7.4 and 8.6 ppm (ImH^+ counterion) in the ^{1}H NMR spectrum of a fresh D_2O solution are consistent with **2**. The absence of characteristic resonances at −21.4, −16.0, and −5.7 ppm[1] confirms that the sample is free of **1**. No other NMR peaks are observed.

[$RuCl_3Im_2$(DMAD)]. A 1:1 solution of DMAD and complex **1** (15 mg) in methanol (25 mL) was stirred for several days. Solvent was removed under vacuum, and the residual solid was washed with cold methanol (2 mL). This solid was then redissolved in a small volume of methanol and allowed to recrystallize over a period of a week. The dark purple powder was filtered, washed with methanol (3 mL), and dried in high vacuum. IR data (CsI, cm^{-1}): 343 (vs), 324 (vs), ν(Ru-Cl); 247 (m), 254 (m), ν(Ru−N); 614 (s), coordinated Im. Anal. Calcd for $C_{13}H_{17}Cl_3N_9Ru \cdot 0.5H_2O$: C, 30.27; H, 3.52; N, 24.44. Found: C, 30.30; H, 3.45; N, 24.47.

Crystallographic Work. X-ray diffraction work on both compounds was carried out with an Enraf-Nonius CAD-4 diffractometer. A reduced cell was determined from 25 reflections on a rotation photograph, and final cell parameters were calculated by least-squares refinement on 25 higher angle reflections ($20° < \theta < 25°$) obtained from a quick precollection. Four standards were used to monitor the intensity every hour and the orientation every 200 measurements. Crystal data for both compounds are given in Table 1.

Structure Determination of [$Ru(OH)_2Im_4$][$RuCl_4Im_2$]. The compound was obtained from a solution of complex **1** (8 mg) in D_2O (2 mL), to which imidazole (either 2 or 20 equiv) was added. The red crystals were filtered and washed with cold water and acetone.

An elongated parallelepiped was used for X-ray work. The Niggli parameters indicated a monoclinic reduced cell. The Laue symmetry ($2/m$) and the systematic absences ($h0l$, $l \neq 2n$; $0k0$, $k \neq 2n$) checked in the intensity data set uniquely identified space group $P2_1/c$. A whole

(11) Toi, H.; La Mar, G. N.; Margalit, R.; Che, C. M. Gray, H. B. *J. Am. Chem. Soc.* **1984**, *106*, 6213.
(12) Clarke, M. J. In *Metal Complexes in Cancer Chemotherapy*; Keppler, B. K., Ed.; VCH: Weinheim, Germany, 1993; pp 129−156, and references cited therein.
(13) Alessio, E.; Milani, B.; Calligaris, M.; Brescian-Pahor, N. *Inorg. Chim. Acta* **1992**, *194*, 85. Alessio, E.; Milani, B.; Mestroni, G.; Calligaris, M.; Faleschini, P.; Attia, W. M. *Inorg. Chim. Acta* **1990**, *177*, 255. Alessio, E.; Xu, Y.; Cauci, S.; Mestroni, G.; Quadrifoglio, F.; Viglino, P.; Marzilli, L. G. *J. Am. Chem. Soc.* **1989**, *111*, 7066. Cauci, S.; Alessio, E.; Mestroni, G.; Quadrifoglio, F. *Inorg. Chim. Acta* **1987**, *137*, 19. Farrell, N.; De Oliveria, N. D. *Inorg. Chim. Acta* **1980**, *66*, L61.
(14) Henn, M.; Alessio, E.; Calligaris, M.; Attia, W. M.; Mestroni, G. *Inorg. Chim. Acta* **1991**, *187*, 39.
(15) Jaswal, J. S.; Rettig, S. J.; James, B. R. *Can. J. Chem.* **1990**, *68*, 1808.
(16) Alessio, E.; Balducci, G.; Calligaris, M.; Costa, G.; Attia, W. M.; Mestroni, G. *Inorg. Chem.* **1991**, *30*, 609.
(17) Alessio, E.; Mestroni, G.; Nardin, G.; Attia, W. M.; Calligaris, M.; Sava, G.; Zorzet, S. *Inorg. Chem.* **1988**, *27*, 4099.
(18) Alessio, E.; Balducci, G.; Lutman, A.; Mestroni, G.; Calligaris, M.; Attia, W. M. *Inorg. Chim. Acta* **1993**, *203*, 205.
(19) Grenier, L.; Charland J. P.; Beauchamp, A. L. *Can. J. Chem.* **1988**, *66*, 1663.
(20) Itaya, T.; Matsumoto, H.; Ogawa, K. *Chem. Pharm. Bull.* **1980**, *28*, 1920.
(21) Harris, T. M.; Randall, J. C. *Chem. Ind. (London)* **1965**, 1728.
(22) Králík, F.; Vrěšťál, J. *Collect. Czech. Chem. Commun.* **1961**, *26*, 1298.

sphere of data (10 162 reflections) was collected by the $\omega/2\theta$ scan technique. Intensity variations remained within ±2.0% during data collection. These data were corrected for absorption (Gaussian integration, grid 10 × 10 × 10; transmission range, 0.076−0.387) and averaged to 2722 independent *hkl* and $\bar{h}kl$ reflections, of which 2435 where above background ($I > 3\sigma_I$). The usual corrections for the effects of Lorentz and polarization were finally applied.

From the Patterson map, the four Ru atoms were found to lie on two sets of crystallographic inversion centers. The remaining atoms were located from structure factor and ΔF calculations. Refinement was done on $|F|$ by full-matrix least-squares procedures. The function minimized was $\sum w(|F_o| - |F_c|)^2$ with individual weights w based on counting statistics ($w = 1/[\sigma^2(F_o) + 0.00005F_o2]$). All non-hydrogen atoms were refined anisotropically. The hydrogens were fixed at idealized positions (C(N)−H = 0.95 Å, $U_{iso} = (U_C + 0.01)$ Å^2). The general background in the final ΔF map was below ±0.3 e Å^{-3}. A few residuals of ±|0.9−1.2| e Å^{-3} remained near the Ru atoms.

Structure Determination of $[RuIm_6]CO_3{\cdot}5H_2O$. Yellow hexagonal crystals appeared within several weeks in the D_2O solution (1 mL) of C(2)-deuterated imidazole (1.5 M) and $(ImH)_2[RuCl_5Im]$ (**2**) (7 mg) used for ^{1}H NMR studies. They were filtered and washed with cold water and acetone.

A hexagonal unit cell was found, and a whole sphere of data (10 322 reflections) was collected as discussed above. The standards varied within ±1.8% during data collection. Comparison of intensities indicated 6/*m* Laue symmetry. The data were averaged to 950 unique reflections, of which 819 were above background. They were corrected for the effects of Lorentz and polarization. Space groups $P6_3$ and $P6_3/m$ were the only ones consistent with the single condition of systematic absences ($00l$, $l \neq 2n$). The structure was solved in the centric $P6_3/m$ space group.

The two Ru atoms in the unit cell had to occupy one of the 2-fold equipoints. Four such equipoints are available in the space group, providing three nonequivalent starting points for structure resolution: 2*a* ($\bar{6}$ symmetry), 2*b* ($\bar{3}$), and 2*c* (or 2*d*, $\bar{6}$). These models were all tested and only when Ru was placed on the origin (2*b*) did a reasonable structure develop. Two CO_3^{2-} were then found on equipoint 2*d*, whereas positions for 10 water molecules were identified: two O(2) on 2*a*, six O(3) on 6*h*, and two O(4) on 2*c*. These atoms were first refined isotropically. In the next ΔF map, the imidazole hydrogens were all visible, and they were introduced as fixed contributors at idealized positions as discussed above. After anisotropic refinement of all non-hydrogen atoms, the thermal ellipsoids of O(3) and O(4) were elongated in the *c* direction and large electron density residuals remained near these atoms, indicating that they did not lie exactly on the crystallographic mirror plane. Thus, they were displaced from the plane, half-occupancies were imposed, and their *z* coordinates were included in the refinement. Hydrogens were positioned as described in the supplementary material. All non-hydrogen atoms were anisotropically refined. The background in the final ΔF map was below ±0.18 e Å^{-3}.

The refined coordinates of the non-hydrogen atoms for both structures are given in Table 2. The temperature factors and hydrogen coordinates are available as supplementary material. All calculations were done with the NRCVAX package.[23]

Results and Discussion

$(ImH)[RuCl_4Im_2]$ (**1**) and $(ImH)_2[RuCl_5Im]$ (**2**) are both obtained by reacting imidazole with activated $RuCl_3$ in HCl/ethanol, and many variations of published procedures[2,8,22,24] were tested to obtain one compound free from the other. Relatively vigorous conditions (high ImH/$RuCl_3$ ratio, heating, long reaction time)[1] are needed to avoid contamination of **1** by the intermediate **2**. Pure **2** was more easily isolated by using less severe conditions (see Experimental Section). In both cases, low acidity was avoided since it led to complex mixtures of **1**, **2**, aquation products, and other unidentified compounds.

The infrared spectrum of **2** matches the results (400−4000 cm^{-1}) published previously.[22] In the metal−ligand region, the spectrum is distinctly different from that of complex **1**. There are three absorptions (308, 287, and 275 cm^{-1}) attributed to Ru−Cl stretching, compared to two for complex **1**, in agreement with the presence of an extra Ru−Cl bond. The weak peak at 255 cm^{-1} could be due to Ru−N stretching.[2] No bands are seen between 310 and 600 cm^{-1}, where Ru−OH_2 or Ru−OH stretching vibrations should appear,[25,26] thereby ruling out the presence of aqua or hydroxo species in the solid sample.

Aqueous Solutions of $(ImH)_2[RuCl_5Im]$. The ^{1}H NMR spectrum of a fresh D_2O solution of **2** (Figure 1a) contains five major peaks. Sharp resonances (7.4 and 8.6 ppm, not shown) for H(2) and H(4)/H(5) protons of the imidazolium ion occur at the same place as for complex **1**.[1] The N−H protons are not seen due to rapid exchange with the solvent. Three broad peaks typical of imidazole coordinated to the paramagnetic Ru(III) center appear at very high field. The narrowest signal at −6.7 ppm is attributed to H(5), the proton furthest from the metal center. Assignment of the −15.0 and −27.0 ppm signals to H(4) and H(2), respectively, is based on experiments with deuterated imidazole (see below).

Although $[RuCl_5Im]^{2-}$ is the species present in the solid, the signals initially observed in the spectrum belong to the aquation product $[RuCl_4(H_2O)Im]^-$ (**2a**).[5] Fast replacement of the first

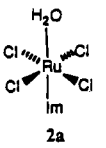

2a

chloride in $[RuCl_5Im]^{2-}$ is anticipated, considering that $[RuCl_5(H_2O)]^{2-}$ is stable only in 6 M HCl and that it aquates within seconds in H_2O.[27] The ^{1}H spectrum of **2** in 6 M NaCl leaves no doubt as to the initial chloride displacement in $[RuCl_5Im]^{2-}$. The fresh solution shows signals for two species: those assigned to **2a** at −6.9, −13.7, and −27.2 ppm (shifted slightly due to high salt concentration, as commonly observed) and an extra set at −3.1, −12.4, and −22.8 ppm, assigned to $[RuCl_5Im]^{2-}$. Spectra taken later showed that the new set of peaks for **2** decreased in favor of those of **2a**, as the monoaqua species formed slowly in the presence of NaCl.

Spectra recorded over several weeks (Figure 1) show that the solution chemistry of **2** is complicated, successive aquation processes competing with coordination of a second imidazole ligand to form **1** (Scheme 1). Within hours (Figure 1b), two sets of peaks barely visible in Figure 1a have become more important. They must be attributed to two separate species since their intensities fit no reasonable stoichiometry and they increase or decrease independently with time. The stronger set (−5.3, −10.9, and −27.0 ppm) is assigned to a $[RuCl_3(H_2O)_2Im]$ species (**2b**) formed from **2a** by further aquation. No clues concerning the stereochemistry of this and other derived species can be extracted from the spectrum, since there is only one coordinated Im ligand. The weaker set of peaks (−6.1, −16.1, and −21.0 ppm) corresponds to the known species **1**, resulting from the replacement of a coordinated water molecule in **2a** by imidazole. The bis(imidazole) complex remains a significant component throughout and does not revert to a monoimidazole

(23) Gabe, E. J.; Le Page, Y.; Charland, J. P.; Lee, F. L. *J. Appl. Crystallogr.* **1989**, *22*, 384.
(24) Souček, J. *Collect. Czech. Chem. Commun.* **1962**, *27*, 960.
(25) Nakamoto, K. *Infrared and Raman Spectra of Inorganic and Coordination Compounds*, 3rd ed.; Wiley: New York; 1978.
(26) Leduc, M.; Beauchamp, A. L. Manuscript in preparation.
(27) Connick, R. E. In *Advances in the Chemistry of the Coordination Complexes;* Kirschner, S., Ed.; Macmillan: New York, 1961; p 15.

Table 2. Refined Coordinates and Equivalent Isotropic Thermal Parameters (Å^2)

atom	x	y	z	B_{eq}[b]
		$[Ru(OH)_2Im_4][RuCl_4Im_2]$		
Ru(1)	0.000	0.000	0.000	2.02(3)
Ru(2)	0.500	0.500	1.000	2.04(3)
Cl(1)	0.38839(13)	0.44456(15)	1.12710(17)	3.00(7)
Cl(2)	0.64354(13)	0.53414(15)	1.19925(17)	3.11(7)
O(1)	0.0900(3)	0.0060(4)	0.1905(4)	2.7(2)
N(11)	0.5641(6)	0.1345(5)	0.9241(7)	4.2(4)
C(12)	0.5247(6)	0.2473(6)	0.8909(7)	3.4(4)
N(13)	0.5455(4)	0.3174(5)	0.9967(5)	2.5(3)
C(14)	0.5995(6)	0.2440(7)	1.1009(7)	3.7(4)
C(15)	0.6110(7)	0.1316(7)	1.0570(9)	4.5(4)
N(21)	−0.2337(5)	−0.2357(6)	0.0649(7)	4.3(3)
C(22)	−0.1636(7)	−0.1981(7)	0.0042(8)	4.1(4)
N(23)	−0.1142(4)	−0.0970(5)	0.0574(5)	2.4(2)
C(24)	−0.1544(6)	−0.0689(6)	0.1589(8)	3.2(3)
C(25)	−0.2293(6)	−0.1544(7)	0.1623(8)	3.7(4)
N(31)	−0.1013(5)	0.3345(5)	0.1235(6)	3.4(3)
C(32)	−0.0430(6)	0.2307(6)	0.1400(7)	3.1(3)
N(33)	−0.0702(4)	0.1642(5)	0.0297(6)	2.5(3)
C(34)	−0.1495(6)	0.2299(7)	−0.0600(7)	3.9(4)
C(35)	−0.1682(7)	0.3346(7)	−0.0022(8)	4.4(4)
		$[RuIm_6]CO_3 \cdot 5H_2O$		
Ru	0.0000	0.0000	0.0000	2.131(12)
O(1)	0.3875(3)	0.8283(3)	0.75000	3.38(14)
O(2)	0.0000	0.0000	0.75000	5.51(19)
O(3)[a]	0.7297(5)	0.0614(5)	0.7649(3)	5.3(3)
O(4)[a]	0.33333	0.66667	0.2720(5)	7.2(6)
C(1)	0.33333	0.66667	0.75000	2.20(15)
N(1)	0.3164(3)	−0.0578(3)	−0.13738(10)	3.64(12)
C(2)	0.1664(3)	−0.0853(3)	−0.11321(11)	3.18(12)
N(3)	0.1898(2)	−0.0036(3)	−0.05786(9)	2.67(10)
C(4)	0.3648(3)	0.0791(4)	−0.04729(13)	4.04(15)
C(5)	0.4427(4)	0.0459(4)	−0.09584(15)	4.70(16)

[a] Occupancy factor = 0.50. [b] B_{eq} is the mean of the principal axes of the thermal ellipsoid.

species, since the Ru−N bond once formed is kinetically inert.[28] The affinity of the monoimidazole system for a second imidazole ligand seems to be high, since the reaction takes place even though the concentrations are very low, the free-imidazole: complex ratio is only 2:1, and most of the free imidazole is quenched as imidazolium ions ($pK_a \sim 7$)[29] whose proton must be displaced upon coordination.

Within 48 h (Figure 1c), all of the original species **2a** has aquated to **2b**, which represents ~75% of the intensity. The bis(imidazole) complex **1** is still present, but the signals of its aquation product $[RuCl_3(H_2O)Im_2]$ (**1a**) are beginning to appear at −4.7, −12.0, and −19.2 ppm. After a period of 3 days (spectrum not shown), a new set of peaks, growing at the expense of those of **2b**, is found (−5.5, −9.3, and −24.5 ppm) for a product of further aquation $[RuCl_2(H_2O)_3Im]^+$ (**2c**) of the monoimidazole system. By this time, **1** has been replaced by **1a**, as expected.[1] Over the next 2 weeks (Figure 1d), complex **2c** slowly formed from **2b**, and after 18 days (Figure 1e) the solution contained **1a**, **2b**, and **2c** in a 3:3:2 ratio, whereas the peaks for the two isomers of **1b** were barely visible.

These results with $[RuCl_5Im]^{2-}$ support our earlier statement, based on $[RuCl_4Im_2]^-$, that there is a qualitative correlation between the aquation processes for the $[RuCl_nIm_{6-n}]^-$ and $[RuCl_n(H_2O)_{6-n}]^-$ systems:[27,30] chloride-rich species aquate

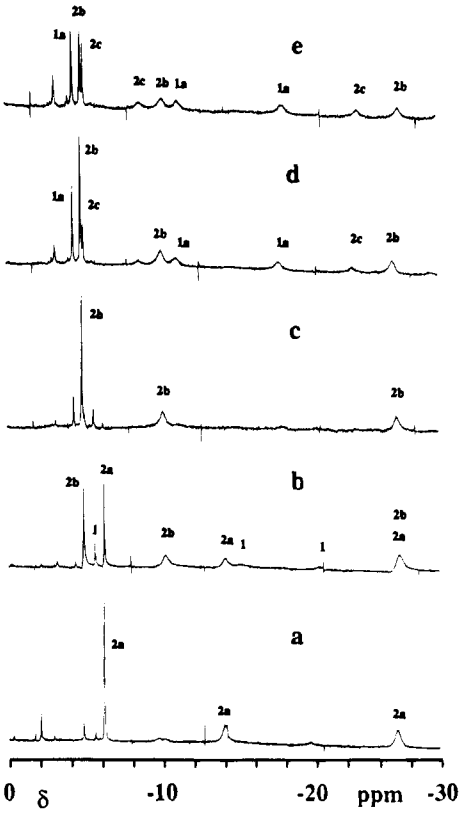

Figure 1. ^1H NMR spectra of complex **2** in D_2O immediately after dissolution (a), after 10 h (b), 2 days (c), 10 days (d), and 18 days (e). Sharp peaks at 7.4 and 8.6 ppm for ImH^+ not shown.

Scheme 1

$$
\begin{array}{lll}
 & & [RuCl_2(H_2O)_2Im_2]^+ \text{ (1b)} \\
 & & \uparrow +H_2O \\
 & & [RuCl_3(H_2O)Im_2] \text{ (1a)} \\
 & & \uparrow +H_2O \\
 & & [RuCl_4Im_2]^- \text{ (1)} \\
 & & \uparrow +Im \\
(ImH)[RuCl_5Im] + H_2O & \longrightarrow & [RuCl_4(H_2O)Im]^- \text{ (2a)} \\
\text{(2)} & & \downarrow +H_2O \\
 & & [RuCl_3(H_2O)_2Im] \text{ (2b)} \\
 & & \downarrow +H_2O \\
 & & [RuCl_2(H_2O)_3Im]^+ \text{ (2c)}
\end{array}
$$

quickly, aquation rates for corresponding steps are similar, and they decrease appreciably for each successive step.

No buffers were added to control pH during these experiments, because side reactions can take place with the buffer material[6,7] during the extended periods of time the solutions are monitored. However, pH was measured regularly. Shortly after dissolution, the pH of a 0.013 M solution of **2** was 4.3, that is, the value expected for a 0.026 M solution of ImH^+ ($pK_a \sim 7$). It had decreased to 3.9 after ~3 h, and it further decreased regularly over the following days, until it stabilized at pH 2.2 after a week. This pattern correlates well with the amount of H^+ ions progressively liberated by the reaction generating $[RuCl_4Im_2]^-$ from $[RuCl_4(H_2O)Im]^-$ and ImH^+.

Reaction of 1 with Imidazole. Adding 2 equiv of imidazole to a D_2O solution of **1** initiated the sequence of reactions depicted in Scheme 2. A pH of 7.0 was initially observed, as expected for an equimolar Im/ImH^+ mixture. After 24 h, the pH had decreased to 6.6 and red crystals of [*trans*-Ru-

(28) Seddon, E. A.; Seddon R. S. *The Chemistry of Ruthenium*, Elsevier: Amsterdam, 1984.
(29) Grimmett, M. R. In *Comprehensive Heterocyclic Chemistry*, Katritzki, A. R., Rees, C. W., Eds.; Pergamon Press: Oxford, U.K., 1984; Vol. 5, Chapter 4.06.
(30) Khan, M. M. T.; Ramachandraiah, G.; Rao, A. P. *Inorg. Chem.* **1986**, *25*, 665.

Scheme 2

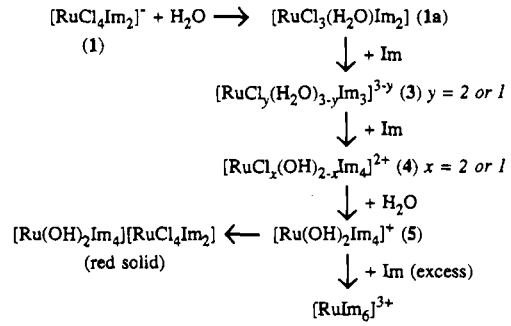

$(OH)_2Im_4][trans\text{-}RuCl_4Im_2]$ (see X-ray work below) had started to appear. Reduction to Ru(II) did not take place, since the ^1H NMR spectra of the mother liquor showed only the sharp peaks for free Im/ImH^+ in fast exchange in the normal aromatic range. In the paramagnetic region (Figure 2a), signals for $[RuCl_4Im_2]^-$ were easily identified and accounted for 20% of the intensity. In the absence of imidazole, ~20% of $[RuCl_4Im_2]^-$ should have already aquated to **1a**,[1] but no signals could be detected for this species here. Instead, two sets of peaks (2:1 ratio) represented altogether 75% of the intensity: H(5) (sharp) at +2.5 and +0.2 ppm, H(2) (broad and overlapping) at −7.8 and −7.0, and H(4) (broad and overlapping) −3.5 and −4.1 ppm. Since the intensity ratio remained constant with time, these peaks were assigned to a species **3** of the type $[RuCl_y(H_2O)_{3-y}Im_3]^{3-y}$ (where some or all H_2O ligands could actually be OH).[5] The *mer* arrangement of Im ligands is preferred, because no evidence for *trans*−*cis* isomerization has ever been found in our earlier studies on the solvolysis of **1**.[1] The value $y = 3$ seems to be ruled out, because our chemical shifts differ from those reported[6] for a species believed to be *mer*-$[RuCl_3Im_3]$. Since full aquation to $[Ru(H_2O)_3Im_3]^{3+}$ should not have occurred at this early stage, species with $y = 2$ or 1 are the most likely possibilities. The spectrum also contained a very weak H(5) signal (5%) at 3.5 ppm for a new species **4** forming at the expense of **3**. During the next few days, **4** was progressively replaced by another species **5**, giving a new strong H(5) peak at 1.2 ppm (H(2) and H(4) probably appear as broad signals at the same place for **3**−**5**).

After 5 days, the precipitation of $[Ru(OH)_2Im_4][RuCl_4Im_2]$ had stopped, the pH had further decreased to 6.2, and the $[RuCl_4Im_2]^-$ signals had disappeared (Figure 2b). The intensities of the free Im/ImH^+ ^1H NMR peaks were then comparable with those of the upfield region, and no Ru(II) species had appeared. The solution still contained some **3**, the relative amount of **4** had increased, but **5** was predominant. Complexes **4** and **5** are probably *trans*-$[RuCl_y(OH)_{2-y}Im_4]^+$ species, since they contain symmetry equivalent Im ligands and only 2 equiv of Im had been added. Complex **5** could be *trans*-$[Ru(OH)_2Im_4]^+$: at this late stage, this ion could accumulate in solution because it is no longer precipitated by $[RuCl_4Im_2]^-$, which has completely disappeared. Species **4** could then be $[RuCl_2Im_4]^+$ or $[RuCl(OH)Im_4]^+$. There is no evidence for higher complexes.

The regular pH decrease (from 7.0 to 6.2) follows the variation of the Im/ImH^+ ratio taking place during these reactions: some of the neutral Im molecules are used to form higher complexes, whereas others become ImH^+ when accepting H^+ ions produced by the precipitation of $[Ru(OH)_2Im_4]^+$ and the aquo−hydroxo equilibria of the soluble species.

A similar experiment was run with a 30-fold excess of imidazole (initial pH 8.5). The first reaction step was not affected appreciably: the peaks of **1** slowly decreased, and red

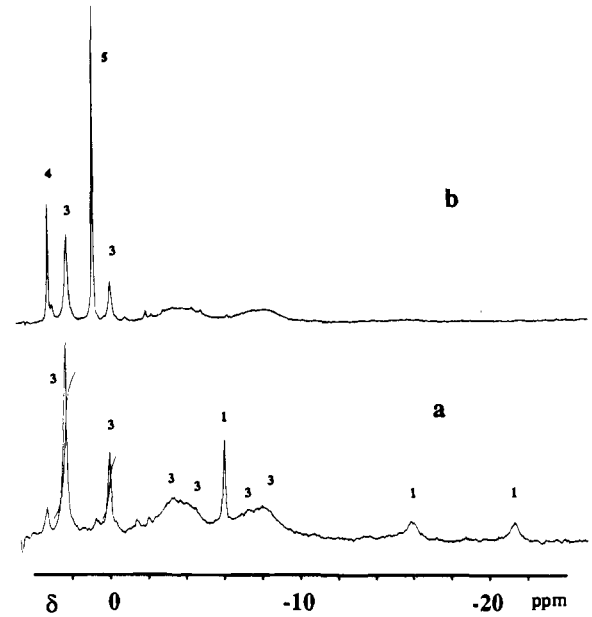

Figure 2. ^1H NMR spectra of D_2O solutions of complex **1** with 2 equiv of imidazole added, after 24 h (a) and 5 days (b).

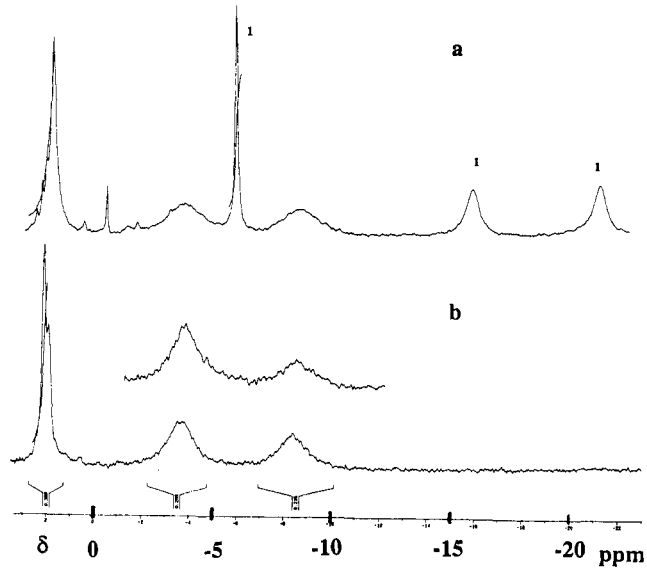

Figure 3. ^1H NMR spectra of D_2O solutions of complex **1** with 30 equiv of imidazole added, after 24 h (a) and after 30 days (b). The inset represents the H(2),H(4) region after 21 days when C(2)-deuterated Im is used.

$[Ru(OH)_2Im_4][RuCl_4Im_2]$ precipitated over several days, as discussed above. During the first few hours, the mother liquor showed very weak signals for **3**−**5**. After 1 day (Figure 3a), these signals were absent and a new set of peaks had appeared (1.6 (H(5)), −3.5 (H(4)), and −8.4 (H(2)) ppm), broader than those of **1** and probably including more than one component. This pattern was retained after **1** had been used up (Figure 3b). The pH stabilized at 8.3, which is consistent with the Im/ImH^+ ratio undergoing only a small variation considering the very large excess of Im used here. The final species in solution could not be identified with certainty, chemical shift values being insensitive to the number of coordinated imidazoles in imidazole-rich molecules (see **3**−**5**, Table 3). However, since all complexes of intermediate composition (like **3**−**5**) not precipitated immediately as $[Ru(OH)_2Im_4][RuCl_4Im_2]$ are quickly jumped over in solution, the final solution likely contains a 5:1 species and/or the fully substituted $[RuIm_6]^{3+}$.

Table 3. ^{1}H NMR Data

complex	H(2)	H(4)	H(5)
1	−21.4	−16.0	−5.7
1a	−19.2	−12.0	−4.7
1b	−17.1	−10.4	−4.4
	−16.0	−6.9	−3.1
1c	−11.7	−7.0	−3.7
2[a]	−22.8	−12.4	−3.1
2a	−27.0	−15.0	−6.7
2b	−27.0	−10.9	−5.3
2c	−24.5	−9.3	−5.5
3	−7.8	−3.5	2.5
	−7.0	−4.1	0.2
4	~−8	~−3	3.5
5	~−8	~−3	1.2

[a] In the presence of 6 M NaCl.

These results show that imidazole has a good affinity for **1**, but the reaction starts slowly. Higher complexes begin to appear roughly at the rate noted earlier for the first aquation step of $[RuCl_4Im_2]^-$ to $[RuCl_3(H_2O)Im_2]$,[1] suggesting that although the aquo species is never observed in the spectra, it probably acts as a short-lived intermediate in which water is quickly replaced by imidazole. The most surprising point is the coexistence, in aged solutions and in the red solid, of the starting $[RuCl_4Im_2]^-$ anion with species having lost most or all of their Cl^- ligands: once the first Cl ligand has been displaced, subsequent substitutions generate imidazole-rich species quickly.

Our earlier results[1,31] on the solvolysis of $[RuCl_4Im_2]^-$ were found to be consistent with a classic dissociative mechanism.[32] The first step here could be similarly controlled, since it is not sensitive to the higher pH and the presence of excess imidazole. However, an accelerating mechanism must come into play for the subsequent steps. A possibility would be a base-catalyzed process of the type found for ammine−cobalt complexes,[33] which could be favored by the higher pH inherent to the presence of excess imidazole. Suitable conjugate-base intermediates could be generated, because our Ru compounds contain acidic protons in the imidazole and aqua ligands: the imidazole N−H protons in $[Ru(NH_3)_5Im]^{3+}$ and those of water in $[Ru(NH_3)_5(H_2O)]^{3+}$ have $pk_a = 8.9$ and 4.1,[34] respectively, and protons with a $pk_a < 7$ are definitely present in Ru(III)−Cl−aqua−Im species.[1]

Crystal Structure of $[Ru(OH)_2Im_4][RuCl_4Im_2]$. The unit cell contains two *trans*-$[RuCl_4Im_2]^-$ and two *trans*-$[Ru(OH)_2Im_4]^+$ (Figure 4), both occupying crystallographic inversion centers. Distances and angles are listed in Table 4.

In both species, departure from octahedral coordination is small. The Ru−N distances (2.075−2.080 Å, $\sigma = 0.005$ Å) compare well with those found in the imidazolium salt of $[RuCl_4Im_2]^-$ [8] and related compounds.[18,35] The Ru−Cl distances (2.360(2) and 2.379(2) Å) are typical of mutually *trans* Ru−Cl bonds in Ru(III) compounds[2,8,15,16,36] and well out of the range (2.40−2.43 Å)[14,15,17] observed for Ru(II) compounds. Thus, the presence of a −1 charge on this species is confirmed, thereby imposing a +1 charge and a Ru(III) center for the $[Ru(OH)_2Im_4]^+$ species, considering that the oxygen-containing ligands can be formally identified as hydroxo groups from the Ru−O bond length: the Ru−O distance of 1.997(4) Å is only slightly longer than that found in *trans*-$[RuCl(OH)py_4]^+$ (1.957(9) Å)[37] but noticeably shorter than those for Ru(III)−OH_2 bonds (2.05−2.10 Å).[26] The geometry of the imidazole ligands is normal.[38]

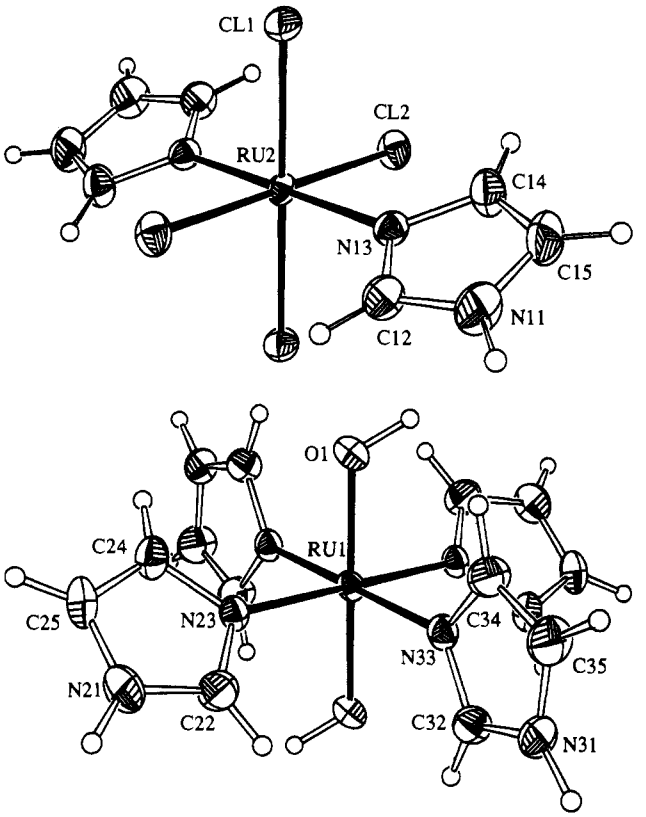

Figure 4. ORTEP drawing of the *trans*-$[RuCl_4Im_2]^-$ (top) and *trans*-$[Ru(OH)_2Im_4]^+$ ions (bottom) in the unit cell of $[Ru(OH)_2Im_4][RuCl_4Im_2]$. In both cases, the Ru atoms occupy crystallographic inversion centers. Ellipsoids correspond to the 50% probability, except for the hydrogen atoms, which are represented as spheres of arbitrary size.

The ions are held in the unit cell by an extended network of hydrogen bonds (Figure 5, supplementary material), which makes this compound insoluble in all common solvents. No ^{1}H NMR data could be obtained. The IR spectrum between 4000 and 600 cm^{-1} is simplified compared with $(ImH)[RuCl_4Im_2]$, since ImH^+ is removed, but some band splitting is still observed because many nonequivalent Im ligands are present. The sharp ν(O−H) peak at 3550 cm^{-1} and the broader ν(N−H) at 3260 cm^{-1} are displaced to 2600 and 2450 cm^{-1}, respectively, by deuteration of these groups. In the 240−600 cm^{-1} region, three main components (341, 332, and 292 cm^{-1}) and a weak feature (357 cm^{-1}) are found in the range normally associated with Ru−Cl stretching. In a region where the chloro−imidazole compounds **1** and **2** show no absorptions, a strong band is found at 512 cm^{-1}, accompanied by a weak component at 534 cm^{-1}. These features must definitely be associated with Ru−(OH) stretching. The frequency is slightly

(31) Anderson, C.; Beauchamp, A. L. *Inorg. Chim. Acta* **1995**, *233*, 33.
(32) Atwood, J. D. *Inorganic and Organometallic Reaction Mechanisms*, Brook/Cole: Montery, CA, 1985; p 76, and references cited therein.
(33) Langford, C. H.; Sasti, V. S. In *Reaction Mechanisms in Inorganic Chemistry*; Tobe, M. L., Ed.; University Park Press: Baltimore, MD, 1972; p 222.
(34) Tweedle, M. F.; Taube, H. *Inorg. Chem.* **1982**, *21*, 3361. Kuehn, C. G.; Taube, H. *J. Am. Chem. Soc.* **1976**, *98*, 689.
(35) Keppler, B. K.; Lipponer, K. G.; Stenzel, B.; Kratz, F. In *Metal Complexes in Cancer Chemotherapy*; Keppler, B. K., Ed.; VCH: Weinheim, Germany, 1993; p 187.
(36) Batista, A. A.; Olmo, L. R. V.; Oliva, G.; Castellano, E. E.; Nascimento O. R. *Inorg. Chim. Acta* **1992**, *202*, 37.
(37) Nagao, H.; Aoyagi, K.; Yukawa, Y.; Howell, F. S.; Mukaida, M. *Bull. Chem. Soc. Jpn.* **1987**, *60*, 3247. Nishimura, H.; Matsuzawa, H.; Togano, T.; Mukaida, M.; Kakihana, H. *J. Chem. Soc., Dalton Trans.* **1990**, 137.
(38) McMullan, R. K.; Epstein, J.; Ruble, J. R.; Craven, B. M. *Acta Crystallogr.* **1979**, *B35*, 688. Hsu, I. N.; Craven, B. M. *Acta Crystallogr.* **1974**, *B30*, 988. Craven, B. M.; McMullan, R. K.; Bell, J. D.; Freeman, H. C. *Acta Crystallogr.* **1977**, *B33*, 2585. Wang, A. C.; Craven, B. M. *Acta Crystallogr.* **1979**, *B35*, 510.

Table 4. Distances and Angles for $[Ru(OH)_2Im_4][RuCl_4Im_2]$

Distances (Å)			
Ru(1)-O(1)	1.997(4)	Ru(2)-Cl(1)	2.360(2)
Ru(1)-N(23)	2.075(5)	Ru(2)-Cl(2)	2.379(2)
Ru(1)-N(33)	2.080(5)	Ru(2)-N(13)	2.078(5)
N(11)-C(12)	1.336(9)	N(23)-C(24)	1.373(9)
N(11)-C(15)	1.351(11)	C(24)-C(25)	1.362(11)
C(12)-N(13)	1.313(9)	N(31)-C(32)	1.345(9)
N(13)-C(14)	1.368(9)	N(31)-C(35)	1.347(11)
C(14)-C(15)	1.334(11)	C(32)-N(33)	1.326(9)
N(21)-C(22)	1.342(10)	N(33)-C(34)	1.371(9)
N(21)-C(25)	1.348(11)	C(34)-C(35)	1.353(11)
C(22)-N(23)	1.311(9)		

Angles (deg)			
O(1)-Ru(1)-O(1)[a]	180.0	Cl(1)-Ru(2)-Cl(1)[b]	180.0
O(1)-Ru(1)-N(23)	88.4(2)	Cl(1)-Ru(2)-Cl(2)	89.58(6)
O(1)-Ru(1)-N(23)[a]	91.6(2)	Cl(1)-Ru(2)-Cl(2)[b]	90.42(6)
O(1)-Ru(1)-N(33)	88.2(2)	Cl(1)-Ru(2)-N(13)	89.9(2)
O(1)-Ru(1)-N(33)[a]	91.8(2)	Cl(1)-Ru(2)-N(13)[b]	90.1(2)
N(23)-Ru(1)-N(23)[a]	180.0	Cl(2)-Ru(2)-Cl(2)[b]	180.0
N(23)-Ru(1)-N(33)	89.8(2)	Cl(2)-Ru(2)-N(13)	90.7(2)
N(23)-Ru(1)-N(33)[a]	90.2(2)	Cl(2)-Ru(2)-N(13)[b]	89.3(2)
N(33)-Ru(1)-N(33)[a]	180.0	N(13)-Ru(2)-N(13)[b]	180.0
C(12)-N(11)-C(15)	108.0(6)	Ru(1)-N(23)-C(24)	127.4(4)
N(11)-C(12)-N(13)	110.5(6)	N(23)-C(24)-C(25)	109.1(6)
C(12)-N(13)-C(14)	105.5(6)	N(21)-C(25)-C(24)	106.6(7)
Ru(2)-N(13)-C(12)	125.9(5)	C(32)-N(31)-C(35)	107.2(6)
Ru(2)-N(13)-C(14)	128.6(5)	N(31)-C(32)-N(33)	111.0(6)
N(13)-C(14)-C(15)	109.0(7)	C(32)-N(33)-C(34)	105.3(6)
N(11)-C(15)-C(14)	106.2(6)	Ru(1)-N(33)-C(32)	126.4(5)
C(22)-N(21)-C(25)	107.3(6)	Ru(1)-N(33)-C(34)	128.2(5)
N(21)-C(22)-N(23)	111.7(7)	N(33)-C(34)-C(35)	109.2(6)
C(22)-N(23)-C(24)	105.4(6)	N(31)-C(35)-C(34)	107.2(6)
Ru(1)-N(23)-C(22)	127.2(5)		

[a] $-x, -y, -z$. [b] $1-x, 1-y, 2-z$.

higher and the bands are sharper than those reported for Ru–OH_2 stretching.[39] A band at 247 cm^{-1}, also found for (ImH)$[RuCl_4Im_2]$, could be due to Ru–N stretching. Other Ru–N modes for $[Ru(OH)_2Im_4]^+$ probably occur at lower frequency.

Reaction of 2 with Imidazole. Excess imidazole (~20 equiv) was added to a D_2O solution of complex **2**. The pH remained constant at 7.8 during this experiment. The ^1H NMR spectrum after 45 min (Figure 6a) shows the known signals for **2a** and **1**, together with a new set (+1.0 (sharp), −3.8 (broad), and −29.5 ppm (broad)) for a species **6**, which is not believed to contain >2 imidazole ligands, because all of the above complexes with ≥3 imidazoles gave broad signals near −4 and −8 ppm. A likely possibility for such a product appearing at an early stage and containing only one type of imidazole is *cis*-$[RuCl_4Im_2]^-$ or a derived aquation product with identical groups *trans* to the imidazoles. Thus, excess imidazole and/or resultant higher pH seems to promote both the formation of the *trans*-$RuIm_2$ species mentioned above and a new substitution pattern leading to *cis*-$RuIm_2$ complexes.

After 24 h, these three species are barely visible (Figure 6b). The dominant features are the very broad resonances near −4 and −9 ppm, typical of imidazole-rich species, accompanied by a number of peaks between −2 and +2 ppm for H(5), one of which (1.9 ppm) is much stronger. After 1 week, this signal is still dominant, and it remains so indefinitely. The spectrum after 6 weeks (Figure 6c) is very similar to that obtained for an aged solution of **1** with excess imidazole (Figure 3b). Therefore, in both systems, a variety of intermediate substitution products

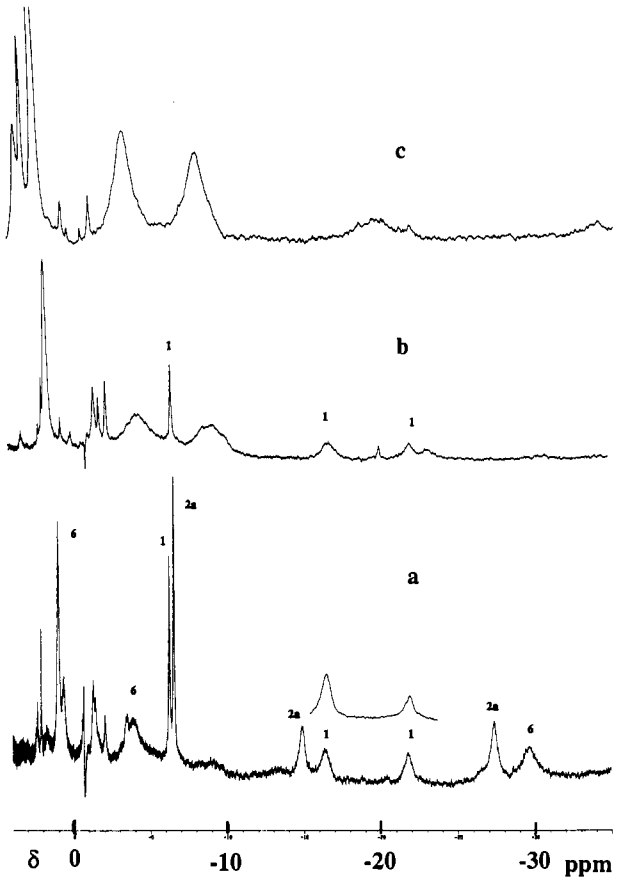

Figure 6. ^1H NMR spectra of D_2O solutions of complex **2** containing ~30 equiv of added imidazole after 45 min (a), 1 day (b), and 40 days (c). The inset in spectrum a was obtained when C(2)-deuterated imidazole was used.

RuX_yIm_{6-y}, with $y \geq 3$ and X = combination of Cl and H_2O/OH, are formed and lead to the fully substituted $[RuIm_6]^{3+}$ as for **1**.

A yellow solid was isolated from aged solutions and shown by X-ray diffraction (see below) to contain the reduced $[RuIm_6]^{2+}$. Whether this and other Ru(II) species are present in solution cannot be determined since their ^1H NMR peaks in the normal region would be obscured by the very strong signals of excess Im/ImH^+. However, $[RuIm_6]^{3+}$ can be presumed to be present in aged solutions.

Reactions of 1 and 2 with C(2)-deuterated Imidazole. Assignment of ^1H Resonances. Assignment of the H(5) proton is straightforward, because its greater distance to the paramagnetic center leads to a relatively sharp peak. However, line width is of no use in identifying the H(2) and H(4) protons, equally distant from the metal.

The above experiments on solutions of **2** were repeated by adding C(2)-deuterated, instead of ordinary, imidazole. As complex **1** appeared, the broad peak at −21 ppm integrated to only ~50% of the other broad peak at −16 ppm (see inset, Figure 6a). Subsequent species resulting from further complexation of C(2)-deuterated imidazole to **2** consistently showed reduced intensity for the peak at higher field. The same trend was also noted for a series of experiments where C(2)-deuterated imidazole was added to solutions of complex **1** (for instance, see inset, Figure 3b). Accordingly, for all spectra in this and our previous work,[1] H(2) was assumed to occur upfield from H(4). These results also confirm that the Ru(III)–N bond is kinetically inert, since the large excess of deuterated imidazole used here would have removed the H(2) signal in a labile system.

(39) Fergusson, J. E.; Greenaway, A. M. *Aust. J. Chem.* **1978**, *31*, 497. Durig, J. R.; McAllister, W. A.; Mercer, E. E. *J. Inorg. Nucl. Chem.* **1967**, *29*, 1441.

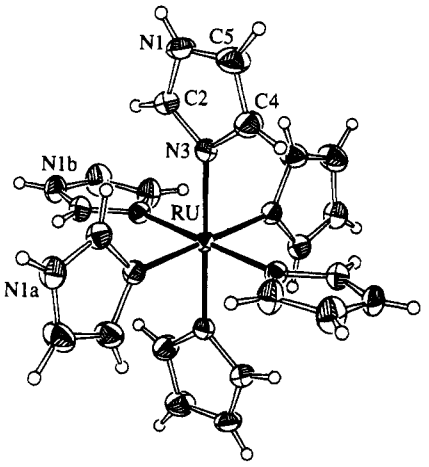

Figure 7. ORTEP drawing of the $[RuIm_6]^{2+}$ cation in $[RuIm_6]CO_3 \cdot 5H_2O$. The three imidazole ligands are related by the 3-fold operation of the crystallographic $\bar{3}$ axis, on which the Ru atom occupies a crystallographic inversion center. Transformations are $a = (-x, x - y, z)$ and $b = (y, -x + y, -z)$. Ellipsoids correspond to 50% probability, except for the hydrogen atoms, which are represented as spheres of arbitrary size.

Table 5. Distances and Angles for $[RuIm_6]CO_3 \cdot 5H_2O$

	Distances (Å)		
Ru–N(3)	2.102(2)	C(2)–N(3)	1.328(3)
C(1)–O(1)	1.279(2)	N(3)–C(4)	1.379(3)
N(1)–C(1)	1.340(3)	C(4)–C(5)	1.347(4)
N(1)–C(5)	1.360(4)		
	Angles (deg)		
N(3)–Ru–N(3)[a]	180.0	C(2)–N(3)–C(4)	105.0(2)
N(3)–Ru–N(3)[b]	90.25(11)	Ru–N(3)–C(2)	127.1(2)
N(3)–Ru–N(3)[c]	89.75(11)	Ru–N(3)–C(4)	127.9(2)
O(1)–C(1)–O(1)	120.0	N(3)–C(4)–C(5)	109.8(2)
C(2)–N(1)–C(5)	107.6(2)	N(1)–C(5)–C(4)	106.5(2)
N(1)–C(2)–N(3)	111.0(2)		

[a] $-x, -y, -z$. [b] $-y, x - y, z$. [c] $y, -x + y, -z$.

Crystal Structure of $[RuIm_6]CO_3 \cdot 5H_2O$. The yellow hexagonal crystals were identified as the CO_3^{2-} salt of the octahedral ruthenium(II) $[RuIm_6]^{2+}$ cation (Figure 7). The anion probably results from absorption of CO_2 from the atmosphere. Distances and angles are listed in Table 5. The metal sits on a site of crystallographic $\bar{3}$ symmetry (3-fold axis and inversion center), making all Im ligands symmetry equivalent and all angles between *trans* bonds equal to 180°. The *cis* angles deviate from 90° by only 0.25°. The Ru–N distance (2.102(2) Å), slightly greater than in the previous structure, reflects mutual steric hindrance between the six ligands. The distances and angles in the Im ligand are similar to those above. The CO_3^{2-} ion occupies a site of crystallographic $\bar{6}$ symmetry (3-fold axis and perpendicular mirror plane): it is therefore perfectly planar, and its angles are rigorously equal to 120°. The C–O distance (1.279(2) Å) is typical of free carbonate ion.[40]

The unit cell (Figure 8, supplementary material) consists of well-separated $[RuIm_6]^{2+}$ ions, interacting via normal van der Waals contacts and forming layers perpendicular to the *c* axis. Halfway between these layers, the CO_3^{2-} ions and water molecules define parallel layers, where they are connected in an extended network of hydrogen bonds (Figure 9, supplementary material).

The crystals are insoluble in all common solvents, so that NMR data could not be obtained.

Reaction of Complex 1 with DMAD. In a previous study,[31] DMAD was found to bind to $[RuCl_4(5\text{-nitroimidazole})_2]^-$ in methanol, especially in aged solution, whereas no reaction was noted in water even after several days. In contrast, complex **1** is found here to react with DMAD, as evidenced from the reaction mixture progressively changing from orange-yellow to very dark purple. The new species shows ^1H NMR signals for three types of DMAD protons (33, 28, and 14 ppm) (Figure 10) with the same pattern as the 5-nitroimidazole species. The first two peaks are assigned to the *N6*-methyl protons, which have become nonequivalent because rotation about the C–NMe_2 bond is slowed down by complexation, as found earlier.[31,41,42] The signal at 14 ppm, with only one-third intensity, is assigned to H(8), because it is absent when C(8)-deuterated DMAD is used. On the high-field side, peaks for coordinated imidazole are located at −2.1, −11, and −16 ppm for H(5), H(4), and H(2), respectively. No resolved signal is detected for the H(2) resonance of DMAD.

Integrations indicate two equivalent Im ligands per coordinated DMAD molecule, in agreement with the $[RuCl_3Im_2(DMAD)]$ formula deduced from microanalysis. Crystals

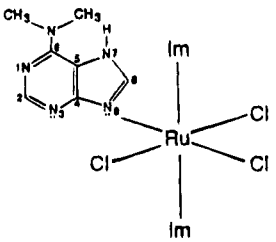

$RuCl_3Im_2(DMAD)$

suitable for X-ray work could not be grown and no clues were provided by the IR spectra. The imidazole ligands are believed to possess the *trans* arrangement, present in the parent complex and apparently retained throughout the solvolytic processes.[1] DMAD is probably present as the N(7)–H tautomer and bonded via N(9), which is the site normally occupied first in metal coordination.[19]

Although its ^1H NMR peaks remained for several weeks, the reaction never reached completion. For instance, after 3 days, a solution of **1** containing 2 equiv of DMAD showed ~25% conversion into the mixed $[RuCl_3Im_2(DMAD)]$ complex, whereas the aquated species **1a** was beginning to appear. This results from the relatively low pH of the solution and the proton-acceptor properties of DMAD. Early in the reaction, the pH of the solution (0.005 M) was ~5.5, and it slowly decreased with time: this is typical of a solution of **1** (without DMAD) slowly forming acidic $[RuCl_3(H_2O)Im_2]$ and other aquated species.[1] However, instead of decreasing to ~3.2, the pH stabilized here at ~4.5 in the presence of DMAD. In addition to raising the final pH, protonation (pk_a of $DMADH^+ = 3.9$)[43] makes DMAD less available for coordination and prevents complete conversion into $[RuCl_3Im_2(DMAD)]$.

The spectrum of Figure 10, obtained after a week in the presence of a large excess (15 equiv) of DMAD, shows an extra pattern of weaker DMAD peaks: two at low field (25.2 and 21.7 ppm) for the methyl groups and one for H(8) at 13.2 ppm. The corresponding imidazole resonances are masked by the stronger signals in the upfield region. This species is probably

(40) Adams, J. M.; Small, R. W. *Acta Crystallogr.* **1974**, *B30*, 2191. Strandberg, R.; Lundberg, B. K. *Acta Chem. Scand.* **1971**, *25*, 1767. Antti, B.; Lundberg, B. K.; Ingri, N. *J. Chem. Soc., Chem. Commun.* **1972**, 712.
(41) Lebuis, A. M.; Beauchamp, A. L. *Inorg. Chim. Acta* **1994**, *216*, 131.
(42) Charland, J. P.; Viet, M. P. T.; St-Jacques, M.; Beauchamp A. L. *J. Am. Chem. Soc.* **1985**, *107*, 8202.
(43) Albert, A.; Brown, D. J. *J. Chem. Soc.* **1954**, 2060.

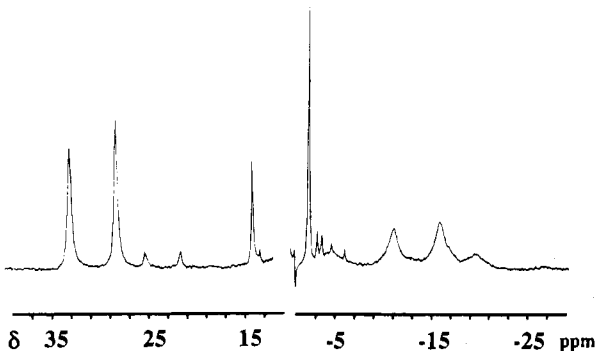

Figure 10. ^{1}H NMR spectrum of a solution of complex **1** in D_2O in presence of 15 equiv of dimethyladenine after 7 days. The 0−12 ppm region containing strong peaks for unreacted DMAD, ImH^+ ions, and the solvent is omitted for simplicity.

a 1:2 Ru/DMAD complex. When lower amounts of DMAD are used, this bis−DMAD species is not detected.

Concluding Remarks

The most obvious difference between **2** and **1** in water solutions is the very high affinity of the former for an extra Im ligand. Under conditions where formation of $[RuCl_3Im_3]$ from $[RuCl_4Im_2]^-$ is not detected, some $[RuCl_4Im_2]^-$ is found to form relatively quickly from $[RuCl_5Im]^{2-}$, even though the only source of imidazole is the ImH^+ ion. It would be interesting to check if the antitumor activity of $(ImH)_2[RuCl_5Im]$ could in fact be that of the small amount of the latter compound formed in situ.

This study also shows that a very different reaction pattern is followed when *non-protonated* imidazole is added to the solution. Although the starting $[RuCl_4Im_2]^-$ is found to change only slowly, as in the absence of neutral imidazole, subsequent substitutions take place at a much faster rate, leading to imidazole-richer species. The structure of $[Ru(OH)_2Im_4][RuCl_4Im_2]$ provides a good illustration of the contrast between the initial slow step allowing $[RuCl_4Im_2]^-$ to survive for a long time and the subsequent fast substitutions to $[Ru(OH)_2Im_4]^+$, where all four Cl^- ligands have been displaced. This unusual kinetic pattern can be ascribed to the higher pH imposed by the presence of excess imidazole. With the less basic DMAD ligand, pH remains lower and no such acceleration is noted: the 1:1 $[RuCl_3Im_2(DMAD)]$ complex forms slowly, a large excess of DMAD does not greatly accelerate the reaction, and only a small amount of a higher complex is found.

Further studies are being planned to fully determine the composition and structure of the various species formed, evaluate their acid−base properties, and understand the reaction mechanism involved, in order to cast more light on the processes taking under biological conditions.

Acknowledgment. We thank M. Simard and F. Bélanger-Gariépy for assistance with the crystallographic part of this work, as well as J. D. Wuest and J. Vaugeois for access to the FTIR instrument. The financial support of the Natural Sciences and Engineering Research Council of Canada is gratefully acknowledged.

Supporting Information Available: Diagrams of unit cells (Figures 5, 8, and 9), tables of anisotropic temperature factors, hydrogen coordinates, least-squares plane calculations, and geometry of hydrogen bonds, and packing diagrams for both structures (15 pages). Ordering information is given on any current masthead page.

IC941244L